

## Magnetic skyrmions and their lattices in triplet superconductors

A. Knigavko

*Department of Electrophysics, National Chiao Tung University, Hsinchu, Taiwan 30050, Republic of China*

B. Rosenstein

*Department of Electrophysics, National Chiao Tung University, Hsinchu, Taiwan 30050, Republic of China  
and National Center for Theoretical Sciences, National Chiao Tung University, Hsinchu, Taiwan 30043, Republic of China*

Y. F. Chen

*Department of Electrophysics, National Chiao Tung University, Hsinchu, Taiwan 30050, Republic of China*

(Received 25 January 1999)

A complete topological classification of solutions in SO(3) symmetric Ginzburg-Landau free energy has been performed and a new class of solutions in weak external magnetic field carrying two units of magnetic flux has been identified. These solutions, magnetic skyrmions, do not have a singular core as Abrikosov vortices do and at low magnetic field they become lighter for strongly type II superconductors. As a consequence, the lower critical magnetic field  $H_{c1}$  is reduced by a factor of  $\ln \kappa$ . Magnetic skyrmions repel each other as  $1/r$  at distances much larger than magnetic penetration depth  $\lambda$  forming a relatively robust triangular lattice. Magnetization near  $H_{c1}$  increases gradually as  $(H - H_{c1})^2$ . This behavior agrees very well with experiments on heavy fermion superconductor UPt<sub>3</sub>. Newly discovered Ru based compounds Sr<sub>2</sub>RuO<sub>4</sub> and Sr<sub>2</sub>YRu<sub>1-x</sub>Cu<sub>x</sub>O<sub>6</sub> are other possible candidates to possess skyrmion lattices. Deviations from exact SO(3) symmetry are also studied. [S0163-1829(99)06425-5]

### I. INTRODUCTION

A rich variety of novel magnetic properties can be found in superconductors with an unconventional type of pairing symmetry. At present several examples of unconventional superconductors are known. The first of them is, of course, a family of  $T_c$  cuprates. In connection with them a lot of recent effort has been devoted to the study of  $d$ -wave pairing of various types with a possible admixture of  $s$  wave. On the other hand, a triplet type of pairing is believed to exist in UPt<sub>3</sub> (Refs. 1,2) and in some other heavy fermion compounds.<sup>3</sup> It is also suspected to occur in recently discovered new classes of Ru based superconductors, layered perovskite Sr<sub>2</sub>RuO<sub>4</sub>,<sup>4,5</sup> and bulk compound Sr<sub>2</sub>YRu<sub>1-x</sub>Cu<sub>x</sub>O<sub>6</sub> (Ref. 6) which has a double perovskite structure. Since all mentioned superconductors are strongly type II, vortices play the major role in their thermodynamical properties. In high- $T_c$  superconductors, despite fundamental differences in mechanism and microscopic properties compared to conventional superconductors, vortices are quite similar to conventional Abrikosov vortices. The reason for this is the existence of a dominant single order parameter field:  $d$ -wave condensate. Small (sometimes quite important) deviations can be accounted for due to the admixture of the  $s$ -wave component. Then, the order parameter is effectively multicomponent. This property leads generally to various new effects such as nonaxisymmetric vortices<sup>7,8</sup> and phase transitions within flux line lattices near  $H_{c2}$ .<sup>9</sup> Similar phenomena exist and should be even more pronounced in systems with an intrinsically multicomponent superconducting order parameter<sup>10,11</sup> such as heavy fermion compounds.

The situation in triplet superconductors might be more exotic. The order parameter is necessarily multicomponent.

In addition, under certain conditions the rotational symmetry (at least an approximate one) between different components might exist. In that case vortices are not the only type of topological solitons which can carry magnetic flux through the sample. The corresponding phenomenological Ginzburg-Landau theory has the order parameter of a vector type with a continuous symmetry. It is known in the theory of superfluid <sup>3</sup>He (Ref. 12) that in such a system there exist topological defects which have no singularities even within the London approximation. On the other hand, vortices have a singularity at their core, at least for one of the components of the order parameter. This makes their energy roughly proportional to  $\ln \kappa$ , similar to the case of a standard Abrikosov vortex. Therefore, for sufficiently large  $\kappa$  vortices are expected to be heavier than nonsingular topological defects and the latter become the most likely candidates for thermodynamically stable configurations of the order parameter field into which a homogeneous superconducting (Meissner) state transforms under the action of an external magnetic field.

It is the purpose of the present paper to investigate this possibility in detail. We find such a nonsingular in the London approximation solution, the magnetic skyrmion, describe its structure, and show that it is energetically favorable over the Abrikosov vortex in a wide range of Ginzburg-Landau parameter  $\kappa$  values. Lattices of magnetic skyrmions are particularly important at fields near the lower critical field. The most striking effects are the reduction of  $H_{c1}$  by a factor of  $\ln \kappa$  and a dramatic change in the behavior of magnetization near  $H_{c1}$ . We also investigate what happens to magnetic skyrmions when the continuous symmetry breaking terms are introduced into the free energy. It is shown that they survive under small perturbations and gradually evolve to

other still nonsingular configurations under large perturbations of a certain type.

Magnetic skyrmion lattices may have already been experimentally observed in  $\text{UPt}_3$ . Magnetization curves near  $H_{c1}$  (Refs. 13,14) are rather unusual (see Fig. 1 of Ref. 15 in which a short account of this work was presented). Theoretically, if the magnetization is due to penetration of vortices into a superconducting sample then one expects  $-4\pi M$  to drop with an infinite derivative at  $H_{c1}$ . On the other hand experimentally  $-4\pi M$  continues to increase smoothly. Such a behavior was attributed to strong flux pinning or surface effects.<sup>13</sup> However, both experimental curves in Fig. 1 of Ref. 15, as well as the other ones found in literature, are close to each other if plotted in units of  $H_{c1}$ . We propose a more fundamental explanation of the universal smooth magnetization curve near  $H_{c1}$ . If one assumes that fluxons are of unconventional type for which interaction is long range then precisely this type of magnetization curve is obtained. Indeed magnetization near  $H_{c1}$  due to fluxons carrying  $N$  units of flux  $\Phi_0 \equiv hc/2e$ , with line energy  $\varepsilon$  and mutual interaction  $V(r)$ , is found by minimizing the Gibbs energy of a very sparse triangular lattice

$$G(B) = \frac{B}{N\Phi_0}[\varepsilon + 3V(a_\Delta)] - \frac{BH}{4\pi}, \quad (1)$$

where  $a_\Delta = (\Phi_0/B\sqrt{3})^{1/2}$  is lattice spacing. When  $V(r) \sim \exp[-\lambda r]$ , the magnetic induction has the conventional behavior  $B \sim [\ln(H - H_{c1})]^{-2}$ ,<sup>16</sup> while if it is long range,  $V(r) \sim 1/r^n$ , then one finds  $B \sim (H - H_{c1})^{n+1}$ . The physical reason for this different behavior is very clear. For a short range repulsion, if one fluxon penetrated the sample, many more can penetrate almost with no additional cost of energy. This leads to the infinite derivative of magnetization. On the other hand for a long range interaction making a place for each additional fluxon becomes energy consuming. Derivative of magnetization thus becomes finite.

The remainder of the paper is organized as follows. In Sec. II we present the  $\text{SO}(3)$  symmetric model and note that it is an excellent approximation to certain successful models of  $\text{UPt}_3$  (Ref. 17) as well as to others.<sup>18</sup> The London approximation is developed. In Sec. III we perform complete topological classification of solutions and find that the magnetic skyrmion carries two units of magnetic flux. General form of cylindrically symmetrical solutions is given. In Sec. IV we determine the magnetic skyrmion lattice structure  $H_{c1}$  and the magnetization curve. An example of deviations from exact  $\text{SO}(3)$  symmetry is considered in Sec. V. More specifically, we address the case of a Zeeman-like interaction relevant to the  $\text{Sr}_2\text{YRu}_{1-x}\text{Cu}_x\text{O}_6$  (Ref. 19) system which initially motivated us to search for exotic vortices. Section VI contains discussion of the results and possibilities to experimentally observe various effects of magnetic skyrmions.

## II. THE MODEL

### A. Ginzburg-Landau free energy functional and its symmetries

Let us consider a model Ginzburg-Landau theory with the order parameter  $\psi_i(\vec{r})$  being a three-dimensional ( $i=1,2,3$ ) complex vector. It is convenient to consider index  $i$  as a spin

in the case of weak spin-orbit coupling in the pairing channel, but this is not a necessary interpretation. The case of the strong-spin-orbit interaction can also be addressed provided some modifications of the free energy functional are made. Average spin of the Cooper pair at a specific point in the space is given by

$$S_i(\vec{r}) \equiv \psi_j^*(\vec{r})(-i\varepsilon_{ijk})\psi_k(\vec{r}). \quad (2)$$

The material under study is assumed to be isotropic. Extensions of our results to anisotropic situations are discussed in Sec. V.

The Ginzburg-Landau free energy functional of the system has the form

$$F = F_{\text{pot}} + F_{\text{grad}} + \frac{1}{8\pi} B_j^2, \quad (3)$$

$$F_{\text{pot}} = -\alpha \psi_i \psi_i^* + \frac{\beta_1}{2} (\psi_i \psi_i^*)^2 + \frac{\beta_2}{2} |\psi_i \psi_i|^2, \quad (4)$$

$$F_{\text{grad}} = \frac{\hbar^2}{2m^*} (\mathcal{D}_j \psi_i)(\mathcal{D}_j \psi_i)^*, \quad (5)$$

where  $\mathcal{D}_j \equiv \partial_j - i(e^*/\hbar c)A_j$  are covariant derivatives,  $B_j \equiv (\nabla \times \mathbf{A})_j$ ,  $m^* > 0$  is the effective mass of the pair, and  $e^*$  is the effective charge of the pair. For a superconducting phase to exist the coefficient  $\alpha$  should be positive below the phase transition point and we set  $\alpha = \alpha'(T_c - T)$  with  $\alpha' > 0$ , while for positive definiteness of the potential the other coefficients of Eq. (4) should satisfy  $\beta_1 > 0$  and  $\beta_2 > -\beta_1$ .

The free energy density Eq. (3) has the following independent symmetries. The spin rotations, forming a group  $\text{SO}_{\text{spin}}(3)$ , act on the index  $i$  of the order parameter field, so that it transforms as a vector. Two-dimensional (orbital) space rotations, forming a different  $\text{SO}_{\text{orbit}}(2)$  group, act on spatial coordinates  $x_j$  and the electric charge transformations, forming a  $\text{U}(1)$  group, rotate the complex phase of the order parameter. Note that in Eq. (3) we assumed that external magnetic field  $\vec{H}$  is oriented along the  $z$  direction. We will consider only configurations invariant under translations in that direction or the thin film geometry.

First we consider the case of zero external magnetic field. Pure superconducting (Meissner) phases that appear below  $T_c$  are found by minimization of  $F_{\text{pot}}$  with respect to  $\psi_i^*$ . This is conveniently done making use of the following parametrization of the order parameter vector:

$$\vec{\psi} = \psi_i \vec{e}_i = f(\vec{n} \cos \phi + i \vec{m} \sin \phi), \quad (6)$$

where  $f > 0$ ,  $0 \leq \phi \leq \pi/2$ ,  $\vec{n}$  and  $\vec{m}$  are unit vectors that are arbitrarily oriented with respect to some fixed coordinate system in the spin space with orthonormal basis  $\vec{e}_1, \vec{e}_2, \vec{e}_3$ . There exist two phases, depending on the sign of the coefficient  $\beta_2$ :

$$\text{I: } \beta_2 > 0, \quad \vec{\psi} = f \frac{\vec{n} + i\vec{m}}{\sqrt{2}}, \quad \vec{n} \perp \vec{m}, \quad \phi = \pi/4, \quad f^2 = \frac{\alpha}{\beta_1}. \quad (7)$$

$$\text{II: } \beta_2 < 0, \quad \vec{\psi} = f e^{i\phi} \vec{n}, \quad \vec{n} = \pm \vec{m}; \quad f^2 = \frac{\alpha}{\beta_1 + \beta_2}. \quad (8)$$

Combining Eqs. (2) and (6) one obtains  $\vec{S} = f^2 \sin 2\phi \vec{l}$ , where  $\vec{l} \equiv \vec{n} \times \vec{m}$ . In phase I the projection of the spin of a Cooper pair  $\vec{S}$  on the vector  $\vec{l}$  is equal to either +1 or -1, reflecting spontaneous time reversal symmetry breaking. In phase II this projection is always zero.

### B. Theories of triplet superconductors and terms breaking $\text{SO}_{\text{spin}}(3)$ symmetry

Obviously, the model of the previous subsection is an idealization of the actual situation in triplet superconductors. In this subsection we note that some successful models of  $\text{UPt}_3$ , notably that of Machida *et al.*,<sup>17</sup> differ from this model only by small less symmetric terms. These terms could be considered as small perturbations, at least in some regions of the  $H$ - $T$  diagram. The asymmetries are of several types. First, the space symmetry  $\text{SO}_{\text{orbit}}(2)$  is normally broken down to some crystallographic point group of a given material ( $D_{6h}$  for  $\text{UPt}_3$ ,  $D_{4h}$  for  $\text{Sr}_2\text{RuO}_4$ ,  $D_{2h}$  for  $\text{Sr}_2\text{YRu}_{1-x}\text{Cu}_x\text{O}_6$ ). The effective mass  $m^*$  then becomes a symmetric tensor  $m_{jk}^*$ . Second, the spin  $\vec{S}$  can be coupled to the magnetic field. This explicitly breaks  $\text{SO}_{\text{spin}}(3)$  down to  $\text{SO}_{\text{spin}}(2)$ . Separate spin and orbital symmetries  $\text{SO}_{\text{spin}}(2) \otimes \text{SO}_{\text{orbit}}(2)$  are broken down to diagonal  $\text{SO}_{\text{tot}}(2)$  as well. The various types of perturbations are

$$\Delta F_{\text{pot}2} = \alpha' [(T_c - T_c^{(1)}) |\psi_1|^2 + (T_c - T_c^{(2)}) |\psi_2|^2], \quad (9a)$$

$$\Delta F_{\text{pot}4} = \beta_3 (|\psi_3|^2 - |\psi_1|^2 - |\psi_2|^2)^2 + \beta_4 |\psi_3|^2 (|\psi_3|^2 - |\psi_1|^2 - |\psi_2|^2), \quad (9b)$$

$$\Delta F_{\text{grad}} = K [(\mathcal{D}_j \psi_i)(\mathcal{D}_i \psi_j)^* + (\mathcal{D}_i \psi_i)(\mathcal{D}_j \psi_j)^*], \quad (9c)$$

$$\Delta F_{\text{Zeeman}} = \mu \vec{S} \cdot \vec{B}, \quad (9d)$$

$$\Delta F_{\text{nonlin}} = \Delta \chi |\vec{\psi} \cdot \vec{B}|^2. \quad (9e)$$

We estimate their coefficients for the case of  $\text{UPt}_3$ . Some models of  $\text{UPt}_3$  do not have three-dimensional complex order parameter and therefore will not be addressed here. Examples include  $E_{1g}$  singlet pairing,<sup>20</sup>  $E_{2g}$  triplet pairing,<sup>21</sup> and the accidental degenerate  $AB$  model.<sup>22</sup> On the other hand, the model of weak spin-orbit coupling developed by Machida *et al.*<sup>17</sup> is of the type we are interested in. In this model asymmetric terms are very important in explaining the double superconducting phase transition at zero external magnetic field. However, they are small in the low-temperature superconducting phase (phase B) well below its critical temperature  $T \ll T_c^- \approx 0.45$  K and at low magnetic fields  $H \approx H_{c1}$ . Indeed, for the quadratic terms one gets from experiment  $(T_c - T_{c1})/T_c \sim 0.2$ ,  $(T_{c1} - T_{c2})/T_c < 0.05$ . The quartic terms Eq. (9b) are an order of magnitude smaller. The corrections to the gradient terms are very small  $K/(\hbar^2/2m^*) \sim 0.01$  and  $\mu/(\hbar^2/2m^*) \sim 0.01$ . The coefficient of the nonlinear coupling term Eq. (9c) is negligible:

$[(\Delta \chi/2)H_{c1}^2]/(\alpha^2/2\beta_1) \approx 10^{-6}$ . Another model of  $\text{UPt}_3$ , which has similar structure to Eq. (3), is the accidental degenerate  $AE$ .<sup>18</sup> Estimates are similar with exception of  $K/(\hbar^2/2m^*)$  which is now of order 1 (found from fitting transition lines near  $H_{c2}$ ).

In general, topological solitons exist even in those cases when the symmetry is weakly broken. In Sec. V we consider in detail the influence of one symmetry breaking term, Zeeman coupling, Eq. (9b), in connection to the material  $\text{Sr}_2\text{YRu}_{1-x}\text{Cu}_x\text{O}_6$ . We show that it does not affect the stability of solitons that we investigate in this paper.

### C. London approximation

The London approximation assumes that the order parameter has the form determined by the potential part of the free energy Eq. (4). In particular, the modulus of the order parameter is fixed. Any variations of the order parameter field over the space are only due to changes of the degeneracy parameters which parametrize the vacuum manifold. From this standpoint in usual  $s$ -wave superconductors there are no topological solitons within the London approximation. The famous Abrikosov vortex has a core—a region in which the modulus of the order parameter varies significantly and vanishes at some point. A vortex can be incorporated into the London approximation at the cost of singularities: the vortex core is assumed to shrink to a point in which energy diverges logarithmically. Accordingly, a cutoff, the correlation length, should be introduced and one obtains  $\ln \kappa$  dependence for a vortex line tension. As discussed above, this means that if there exists a nonsingular solution it is bound to become energetically favorable for  $\kappa$  large enough.

Below we concentrate on the properties of nonunitary phase I, Eq. (7), of a triplet superconductor near the lower critical field  $H_{c1}$ . This phase is always assumed when we refer to the superconducting state. We define magnetic penetration depth  $\lambda \equiv c/|e^*| \sqrt{\beta_1 m^*/4\pi\alpha}$ , coherence length  $\xi \equiv \hbar/\sqrt{2\alpha m^*}$ , flux quantum  $\Phi_0 \equiv hc/e^*$ , and Ginzburg-Landau parameter  $\kappa \equiv \lambda/\xi$ . For convenience we express all physical quantities in dimensionless units as follows:

$$x \equiv \lambda \tilde{x}, \quad F \equiv \frac{\alpha^2}{\beta_1 \kappa^2} \tilde{F}, \quad f^2 \equiv \frac{\alpha}{\beta_1} \tilde{f}^2,$$

$$A \equiv \frac{\Phi_0}{2\pi\lambda} a, \quad B \equiv \frac{\Phi_0}{2\pi\lambda^2} b. \quad (10)$$

The tildes will be omitted hereafter.

In order to determine the degeneracy parameters we consider the symmetry breaking pattern of the superconducting state. Both the spin rotation  $\text{SO}_{\text{spin}}(3)$  symmetry and the superconducting phase  $U(1)$  symmetry are spontaneously broken, but a diagonal subgroup  $U(1)$  survives. It consists of combined transformations: rotations by angle  $\vartheta$  around the axis  $\vec{l}$  which are accompanied by gauge transformations  $e^{i\vartheta}$ . These combined transformations together with rotations of vector  $\vec{l}$  itself, form the vacuum manifold. The vacuum manifold is isomorphic to the  $\text{SO}(3)$  group. Our aim is to find nonsingular topological line defects in this case. We

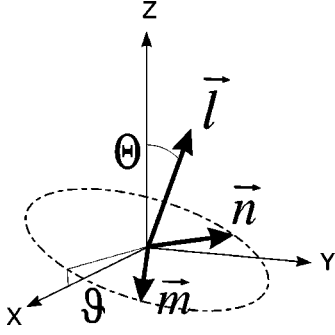


FIG. 1. Definition of angles  $\vartheta$  and  $\Theta$ . Unit vectors  $\vec{l}$ ,  $\vec{n}$ ,  $\vec{m}$  constitute a triad of perpendicular vectors in the spin space.  $\vartheta$  is the superconducting phase defined in Eq. (16).

choose a triad of orthonormal vectors  $\vec{n}$ ,  $\vec{m}$ ,  $\vec{l}$  to be the degeneracy parameters. From the definition of these vectors the following important relations can be derived:

$$\vec{n}\partial_i\vec{m} = -\vec{m}\partial_i\vec{n}, \quad (11)$$

$$(\partial_i\vec{n})^2 + (\partial_i\vec{m})^2 = 2(\vec{n}\partial_i\vec{m})^2 + (\partial_i\vec{l})^2, \quad (12)$$

$$\varepsilon_{pqs}l_p(\partial_i l_q)(\partial_j l_s) = (\partial_i n_p)(\partial_j m_p) - (\partial_i m_p)(\partial_j n_p). \quad (13)$$

To obtain the free energy density of the London approximation we substitute  $\vec{\psi}$  in the form Eq. (7) into the gradient part, Eq. (5), of the total free energy functional and make use of Eqs. (11) and (12). After some algebra we get

$$F_L = \frac{1}{2}(\partial_i\vec{l})^2 + (\vec{n}\partial_i\vec{m} - a_i)^2 + b_i^2. \quad (14)$$

Varying energy functional with respect to vector potential  $\vec{a}$  one obtains the supercurrent equation

$$n_p\vec{\nabla}m_p - \vec{a} = \vec{\nabla} \times (\vec{\nabla} \times \vec{a}) = \vec{j}, \quad (15)$$

where the Maxwell equation was used. Equation (15) shows that the superconducting velocity (in units of  $\hbar/m^*$ ) is given by

$$n_p\vec{\nabla}m_p = -\vec{\nabla}\vartheta. \quad (16)$$

Thus, the angle  $\vartheta$ , which specifies the position the pair of perpendicular unit vectors  $\vec{n}$  and  $\vec{m}$  in the plane normal to vector  $\vec{l}$ , takes the role of superconducting phase in the present case (see Fig. 1). Other field equations are most easily obtained by considering  $F_L(\vec{l}, \vec{n}, \vec{m})$  as a functional of  $\vec{l}$  and  $\vec{n}$  only and performing conditional variation with constraints  $\vec{l} \cdot \vec{n} = 0$ ,  $\vec{l}^2 = \vec{n}^2 = 1$ . This procedure yields the independent equation for  $\vec{l}$

$$\Delta\vec{l} - \vec{l}(\vec{l} \cdot \Delta\vec{l}) + 2j_k(\vec{l} \times \partial_k\vec{l}) = 0. \quad (17)$$

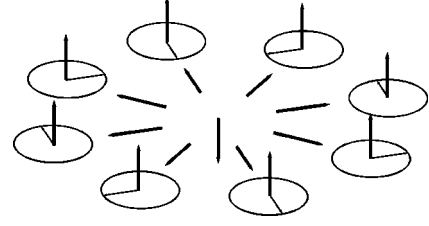


FIG. 2. Configuration of a magnetic skyrmion with  $Q = -1$ . Solid arrows represent  $\vec{l}$  field while ‘‘clocks’’ show that phase  $\vartheta$  rotates twice clockwise as a round on the remote contour is completed.

### III. TOPOLOGICAL CLASSIFICATION OF SOLUTIONS IN LONDON APPROXIMATION

In this subsection we develop a classification scheme for the finite energy solutions to our model in the London approximation derived above. The main result is that the London equations (15) and (17) in the presence of the magnetic flux admit nonsingular topologically stable solutions. This class of solutions contains cylindrically symmetric ones.

#### A. General topological analysis

Let us consider boundary conditions for a superconductor which extends over the whole space. The free energy density Eq. (14) is positive definite and contains  $\vec{B}^2$  term. It follows that magnetic field vanishes at spatial infinity. Then one has to specify the triad  $\vec{n}$ ,  $\vec{m}$ ,  $\vec{l}$  at different distant points. The corresponding (first) homotopy group of vacuum manifold is  $\pi_1[\text{SO}(3)] = \mathbb{Z}_2$ .<sup>12</sup> It yields a classification of finite energy solutions into two topologically distinct classes. This classification is too weak, however, because it does not guarantee nontrivial flux penetrating the plane. We will see that configurations having both ‘‘parities’’ are of interest.

In the presence of the magnetic flux, the configurations are further constrained due to the flux quantization condition. The vacuum manifold is naturally divided into  $\text{SO}(3) \rightarrow \text{SO}(2) \otimes S_2$ , where the  $S_2$  is the direction of  $\vec{l}$  and the  $\text{SO}(2)$  is the superconducting phase  $\vartheta$  defined in Eq. (16). For given number of flux quanta  $N \equiv \Phi/\Phi_0$ , the phase  $\vartheta$  makes  $N$  winds at infinity, see Fig. 2. The first homotopy group of this part is therefore fixed:  $\pi_1[\text{SO}(2)] = \mathbb{Z}$ . If, in addition, vector  $\vec{l}$  is fixed throughout the volume of a superconductor there is no way to avoid singularity in the phase  $\vartheta$ . It becomes ill defined at some point and, accordingly, the modulus of the order parameter have to vanish there. Destruction of the superconducting state takes place in rather small area, especially for large  $\kappa$ . Thus, we arrive at the usual picture of the Abrikosov vortex.

However, the general requirement that a solution has finite energy is much weaker. It tells us that the direction of  $\vec{l}$  should be fixed only at infinity. This follows from the presence of the  $(\partial_i\vec{l})^2$  term in  $F_L$  [see Eq. (14)] which cannot be ‘‘gauged away’’ as the corresponding term for the  $\text{SO}(2)$  part. A relevant homotopy group is  $\pi_2(S_2) = \mathbb{Z}$ . The second homotopy group appears because the constancy of  $\vec{l}$  at infinity (say, up) effectively ‘‘compactifies’’ the two-dimensional physical space into  $S_2$ . One can have topologically nontrivial

configuration, skyrmions, which are markedly different from vortices. Unit vector  $\vec{l}$  can nontrivially wind towards the center of the texture. The topological number  $Q$  should be introduced,<sup>23</sup>

$$Q = \frac{1}{8\pi} \int \varepsilon_{ij} \vec{l} (\partial_i \vec{l} \times \partial_j \vec{l}) dS. \quad (18)$$

Configurations of the order parameter field with topological number  $Q = -1$  ( $Q = +1$ ) have vector  $\vec{l}$  flipping its direction from up to down (or from down to up) until it reaches the center of the texture from an infinitely remote point (see Fig. 2).

To summarize, configurations fall into classes characterized by two integers  $N$  and  $Q$ . The ‘‘parity’’ of the more general topological analysis is just  $Q = N \pmod{2}$ . Due to the presence of two topological numbers an interesting possibility arises. There exists topologically nontrivial configuration that preserves the modulus of the order parameter [see Eq. (7)] at every point. We call these regular solutions magnetic skyrmions. For them these two topological numbers are related to each other. We find this relation integrating the supercurrent equation (15) along a remote contour and using of the identity (13):

$$Q = N/2. \quad (19)$$

The lowest energy solution within the London approximation corresponds to  $N/2 = Q = \pm 1$ .

### B. Cylindrically symmetric magnetic skyrmions

In the class of solution  $N/2 = Q = -1$  there are ones possessing cylindrical symmetry. We will describe them in polar coordinates  $\rho$  and  $\varphi$ . The triad  $\vec{n}$ ,  $\vec{m}$ ,  $\vec{l}$  has the form

$$\begin{aligned} \vec{l} &= \vec{e}_z \cos \Theta(\rho) + \vec{e}_\rho \sin \Theta(\rho), \\ \vec{n} &= [\vec{e}_z \sin \Theta(\rho) - \vec{e}_\rho \cos \Theta(\rho)] \sin \varphi + \vec{e}_\varphi \cos \varphi, \quad (20) \\ \vec{m} &= [\vec{e}_z \sin \Theta(\rho) - \vec{e}_\rho \cos \Theta(\rho)] \cos \varphi - \vec{e}_\varphi \sin \varphi, \end{aligned}$$

where  $\Theta$  is the azimuthal angle of  $\vec{l}$  (see Fig. 1). This choice corresponds to the situation when the pair of perpendicular vectors  $\vec{n}$  and  $\vec{m}$  winds twice as a distant circle on Fig. 2 is completed. Due to cylindrical symmetry of the solution in question function  $\Theta(\rho)$  satisfies boundary conditions  $\Theta = \pi$  at  $\rho = 0$  and  $\Theta = 0$  at  $\rho \rightarrow \infty$ .

The free energy of the magnetic skyrmion per unit length takes the form

$$\epsilon_{ms} = \epsilon_s + \epsilon_{\text{cur}} + \epsilon_{\text{mag}}, \quad (21)$$

$$\epsilon_s \equiv \int \rho d\rho \left[ \frac{1}{2} \left( \frac{d\Theta}{d\rho} \right)^2 + \frac{\sin^2 \Theta}{2\rho^2} \right], \quad (22)$$

$$\epsilon_{\text{cur}} \equiv \int \rho d\rho \left( \frac{1 + \cos \Theta}{\rho} + a \right)^2, \quad (23)$$

$$\epsilon_{\text{mag}} \equiv \int \rho d\rho B^2 = \int \rho d\rho \left( \frac{a}{\rho} + \frac{da}{d\rho} \right)^2, \quad (24)$$

where energy is measured in units of  $\epsilon_0 = (\Phi_0/4\pi\lambda)^2$ . The first part  $\epsilon_{ms}$  is the same as in standard nonlinear  $\sigma$  model without magnetic field.<sup>23</sup> The second term  $\epsilon_{\text{cur}}$  is analogous to the supercurrent contribution in the London approximation of the usual superconductor.<sup>16</sup> The third term is the magnetic energy. Equation (23) shows that a singularity at  $\rho = 0$  is absent (integrand converges) since  $1 + \cos \Theta(0) = 0$ .

The actual distribution of magnetic field and order parameter in this case can be found from the following system of equations:

$$\Theta'' + \frac{1}{\rho} \Theta' = - \frac{\sin \Theta}{\rho} \left( \frac{2 + \cos \Theta}{\rho} + 2a \right), \quad (25)$$

$$a'' + \frac{a'}{\rho} - \frac{a}{\rho^2} - a = \frac{1}{\rho} (1 + \cos \Theta). \quad (26)$$

In the next section we solve this equation.

## IV. MAGNETIC SKYRMION SOLUTION

### A. Blow up of single skyrmion by magnetic field

The general form of the solution of Eqs. (25) and (26) is given in Fig. 2. The orientation of the unit vector  $\vec{l}$  (solid arrows) forms a skyrmion of SO(3) invariant  $\sigma$  model.<sup>23</sup> The phase  $\vartheta$  makes two rounds at infinity (clock inside small circles on the ‘‘infinitely remote’’ circle). If magnetic field were absent there are infinitely many degenerate solutions

$$\Theta_s(\rho) = 2 \arctan(\delta/\rho) \quad (27)$$

which have the same energy  $\epsilon = 2$  for any size of the skyrmion  $\delta$ . The skyrmion of the nonlinear  $\sigma$  model possesses a scale invariance. This degeneracy in various physical problem is lifted by perturbations. In some physical situations the skyrmion is stabilized by four derivative terms,<sup>23</sup> sometimes it shrinks and sometimes blows up. In the present context the magnetic field lifts the degeneracy and we prove below that the skyrmion blows up. Of course if there are many skyrmions present, their repulsion will stabilize the system. This is discussed in the next subsection.

To prove that the skyrmion blows up, we explicitly construct variational configurations and show that as the size of these configurations increases, the energy is reduced to a value arbitrarily close to the absolute minimum of  $\epsilon_{ms} = 2$ . The first term in the energy Eq. (21)  $\epsilon_s$  is the usual expression for the energy of the skyrmion. It is bound from below by the energy of usual skyrmion  $\epsilon = 2$ . To construct a variational configuration for  $\Theta$ , we pick up one of these solutions Eq. (27) of certain size  $\delta$ . The second term  $\epsilon_{\text{cur}}$ , the ‘‘supercurrent’’ contribution is positive definite. Therefore its minimum cannot be lower than zero. One still can maintain the zero value of this term when the field  $\Theta$  is a skyrmion. Assuming this one gets the relation between  $a$  and  $\Theta$ :  $a(\rho) = -(1 + \cos \Theta)/\rho = -2\rho/(\rho^2 + \delta^2)$ . The magnetic field contribution (which is also positive definite) for such a vector potential is  $\epsilon_{\text{mag}} = 8/3\delta^2$ . To sum up, the energy of the configuration is  $\epsilon = 2 + 8/3\delta^2$ . It is clear that when  $\delta \rightarrow \infty$ , we obtain energy arbitrarily close to the lower bound of  $\epsilon = 2$ . The skyrmion therefore blows up.

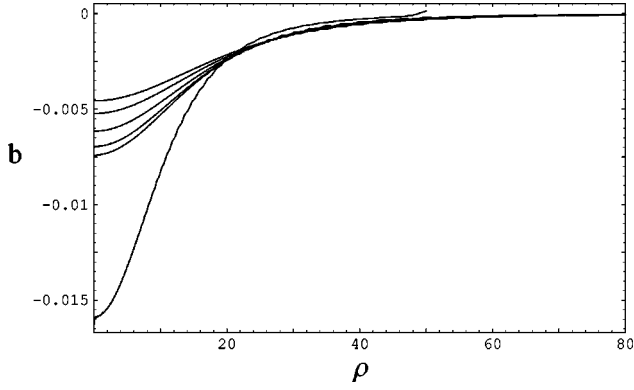


FIG. 3. Magnetic field of the isolated magnetic skyrmion. The distance from the center  $\rho$  varies from 0 to a cutoff  $\rho_{\max}$  with boundary conditions  $(\Theta' + \Theta/\rho)|_{\rho=\rho_{\max}}=0, b|_{\rho=\rho_{\max}}=0$  imitating the infinite domain.  $\rho_{\max}=40\lambda$  for the lowest curve and 600 for the uppermost one.

We also solved Eqs. (25),(26) numerically on the segment of  $\rho$  from 0 to a cutoff  $\rho_{\max}$  with boundary conditions  $b|_{\rho=\rho_{\max}}=0$  and  $(\Theta' + \Theta/\rho)|_{\rho=\rho_{\max}}=0$ . The second boundary condition allows us to approach the correct asymptotic behavior of  $\Theta$  at infinity  $\sim 1/\rho$  which follows from Eqs. (25),(26). The results for the distribution of magnetic field for  $\rho_{\max}$  ranging from 50 to 600 are presented in Fig. 3. One clearly sees that as the cutoff increases the magnetic field at the center  $\rho=0$  decreases and the flux spreads out over larger area. This is in accord with the variational proof above.

### B. Skyrmion lattice and $H_{c1}$

Skyrmions repel each other, as we will see shortly, and therefore form a lattice. Since they are axially symmetric objects, the interaction is axially symmetric and hexagonal lattice is expected (see Fig. 4). Assume that lattice spacing is  $a_{\Delta}$ . At the boundaries of the hexagonal unit cells the angle  $\Theta$  is zero, while at the centers it is  $\pi$ . Magnetic field  $b$  is continuous on the boundaries. Therefore, to analyze magnetic skyrmion lattice we should solve Eqs. (25),(26) on the unit cell with such boundary conditions demanding that two units of flux pass through the cell (by adjusting the value of

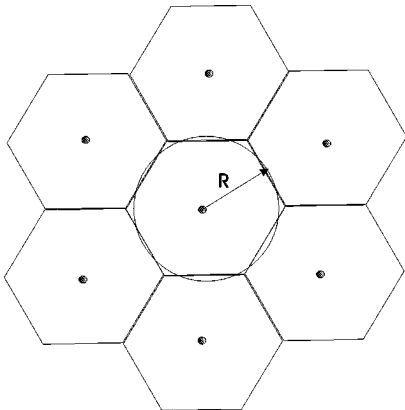


FIG. 4. A fragment of the magnetic skyrmion lattice. For numerical calculations we approximate the symmetric unit cell by a disk of the same area:  $R=(3^{1/4}/\sqrt{2\pi})a_{\Delta}$ .

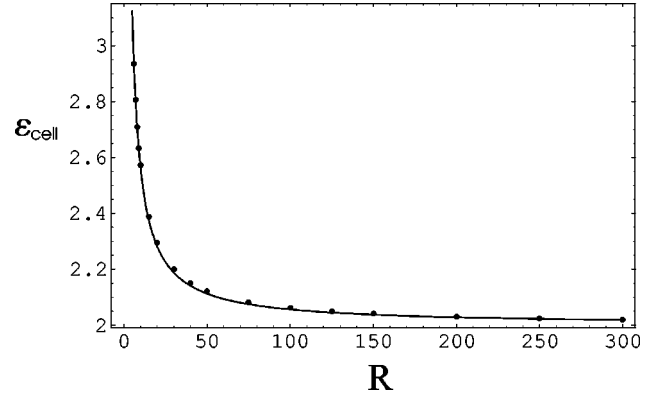


FIG. 5. Energy of the unit cell of the magnetic skyrmion lattice. Dots are numerical values for different  $R$ . The line is the fit of Eq. (28).

magnetic field on the boundary). We approximate the hexagonal unit cell by a circle of radius  $R=(3^{1/4}/\sqrt{2\pi})a_{\Delta}$  having the same area, Fig. 4.

We performed such calculations for  $R$  from  $R=5$  until  $R=600$  using the finite elements method. The result is presented in Fig. 5. The energy per unit cell is described well in a wide range of  $R$  (deviation at  $R=10$  is 1%) by an approximate expression

$$\varepsilon_{\text{cell}}=2+\frac{5.62}{R}. \quad (28)$$

The dominant constant contribution to the energy at large  $R$  comes, as in the analytical variational state, above from the first term  $\varepsilon_s$  in the integrand of Eq. (21). The contribution to the energy Eq. (21) from the supercurrent term  $\varepsilon_{\text{cur}}$  is small for large  $R$  but becomes significant at denser lattices. The third term, magnetic energy  $\varepsilon_{\text{mag}}$  yields a small deviation of magnetic skyrmion energy from 2 at large  $R$ .

Profile of the angle  $\Theta(\rho)$  and of the magnetic field  $b$  are depicted in Figs. 6(a) and 6(b), respectively. Radius of the circular cell  $R$  varies from  $20\lambda$  to  $300\lambda$ . In Fig. 6(a) a smaller value of  $R$  corresponds to a lower curve. Small  $\rho$  asymptotics of the solution up to  $\rho^3$  terms read

$$\Theta(\rho)\rightarrow\pi+c\rho\left[1+\frac{\rho^2}{8}\left(b(0)+\frac{c^2}{3}\right)\right],$$

$$a(\rho)\rightarrow\frac{b(0)}{2}\rho+\frac{\rho^3}{16}[b(0)+c^2],$$

where  $c$  and  $b(0)$  are constants to be determined by numerical integration. Most of the flux goes through the region where the vector  $\vec{l}$  is oriented upwards. In other words, the magnetic field is concentrated close to the center of a magnetic skyrmion.

The value of  $h_{c1}(R\rightarrow\infty)=\varepsilon_{ms}(R\rightarrow\infty)/4$  for a triplet superconductor filling the whole space is equal to 1/2. In physical units this result reads

$$H_{c1}=\frac{\Phi_0}{4\pi\lambda^2}. \quad (29)$$

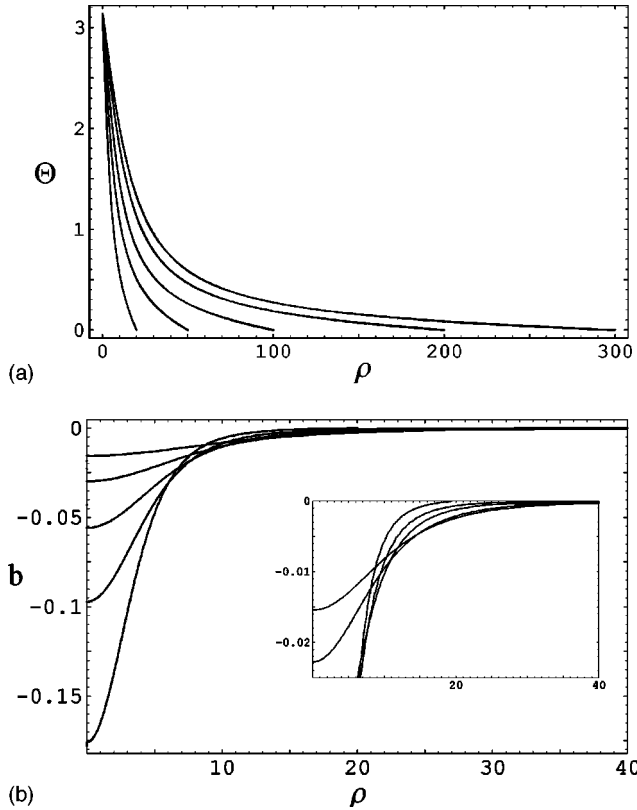


FIG. 6. Numerical solution of GL equations in London approximation for a unit cell of the magnetic skyrmion lattice. Radius of the circular cell  $R$  varies from  $20\lambda$  to  $300\lambda$ . (a) Angle  $\Theta$  as a function of the distance  $\rho$  from the center of the cell. (b) Magnetic field  $b$  as a function of the distance  $\rho$  from the center of the cell. A smaller  $R$  corresponds to a lower curve.

It is quite different from  $H_{c1}$  of conventional ( $s$ -wave) superconductors where an additional factor  $\ln \kappa$  is present. Line energy of Abrikosov vortices  $\varepsilon_v$  for the present model was calculated numerically (beyond London approximation) in Ref. 19. For  $\kappa=20$  and  $50$  we obtain  $2\varepsilon_v/\varepsilon_{ms} \approx 3.5$  and  $4.4$ , respectively. Therefore we expect that the lower critical field of  $\text{UPt}_3$  is determined by magnetic skyrmions.

### C. Magnetization of the skyrmion lattice

If  $h > h_{c1}$  the external magnetic field enforces a definite value of magnetic flux through a sample. Magnetic skyrmions, being topological objects, carry quantized magnetic flux and their number in the sample is determined by the average magnetic induction  $b$ , similarly to the case of vortices. Energy of magnetic skyrmions as function of  $R$  Eq. (28) actually determines the interaction between them. However, magnetic skyrmions, contrary to vortices, are extended objects and their linear size  $R$  is also determined by the number of them in the sample.

To qualitatively estimate the magnetization curve produced by “skyrmion mixed state” we make use of the unit cell energy obtained in the previous section. The Gibbs energy density of the sample of volume  $V=S \times L$ , where  $S$  is the transverse area and  $L$  is longitudinal extension, is given in dimensionless units Eq. (10) by

$$G(b) = \frac{N\varepsilon_{\text{cell}}L}{V} - 2bh = \frac{b}{2} \left( 2 + 5.62 \frac{\sqrt{b}}{2} \right) - 2bh. \quad (30)$$

The second equality follows the facts that magnetic induction  $b$  is related both to the number of magnetic skyrmions  $N=Sb/2$  and to the size of the magnetic skyrmion defined above  $R^2=4/b$ . Minimization of Eq. (30) with respect to  $b$  yields

$$b \approx 0.225 \left( \frac{h}{h_{c1}} - 1 \right)^2, \quad h \geq h_{c1} = \frac{1}{2}. \quad (31)$$

Equation (31) shows that a skyrmion lattice is characterized by zero slope of magnetization curve at  $h_{c1}$ , in contrast to the infinite slope for the magnetization curve associated with a vortex lattice. This circumstance provides a tool in the experimental search for the triplet superconductivity with approximate  $\text{SO}(3)$  symmetry. Our results agree well with the earlier work of Burlachkov *et al.*<sup>25</sup> who also obtained zero slope of the magnetization at  $h_{c1}$  for a stripe  $\vec{l}$  texture which might arise in the case of very high anisotropy of effective mass tensor  $m^*$  [see Eq. (3)].

### V. INFLUENCE OF $\text{SO}(3)$ BREAKING TERMS

In this section we consider influence of an  $\text{SO}(3)$  symmetry breaking terms on skyrmion lattice. List of these terms was given in Sec. IIB Eqs. (9a)–(9e). The perturbations are not expected to affect the existence of topological solitons—just modify their energy. When the coefficient of a breaking term becomes of order 1, the soliton might disappear, although it is not necessary. We study in detail the influence of Zeeman term Eq. (9d). The choice is motivated by our previous study of possible spontaneous vortex state in a new bulk perovskite superconductor  $\text{Sr}_2\text{YRu}_{1-x}\text{Cu}_x\text{O}_6$ .<sup>19</sup>

This compound has very unusual magnetic properties and is suspected to be a  $p$ -wave superconductor for the following reasons.<sup>6</sup> At the temperature of about 60 K, at which superconductivity sets in, these materials begin to exhibit basic ferromagnetic properties such as a hysteresis loop. Experimental observation of a positive remanence suggests existence of spontaneous magnetization in the absence of an external magnetic field. Exact overlap of superconductivity and ferromagnetism lead us to consider an isotropic triplet model Eqs. (3)–(5) in nonunitary phase with spontaneous time reversal symmetry breaking. In this case, a direct spin coupling of the condensate to a magnetic field

$$\mu \vec{S} \cdot \vec{B} = \frac{e^* \hbar}{2m^* c} g \vec{S} \cdot \vec{B} \quad (32)$$

becomes relevant. In what follows this coupling will be referred to as Zeeman-like coupling and characterized by dimensionless parameter  $g$ . For sufficiently large values of  $g$  energetics of the triplet superconductor changes considerably. There exists a critical value  $g_{c1}=1$  above which the mixed state might respond on an external magnetic field ferromagnetically and, on the other hand, in the presence of an external magnetic the field mixed state might occur even for temperatures above  $T_c$ .<sup>19</sup> For larger Zeeman-like coupling,  $g > g_{c2} \approx \ln \kappa$ , vortex energy becomes negative. Spontaneous

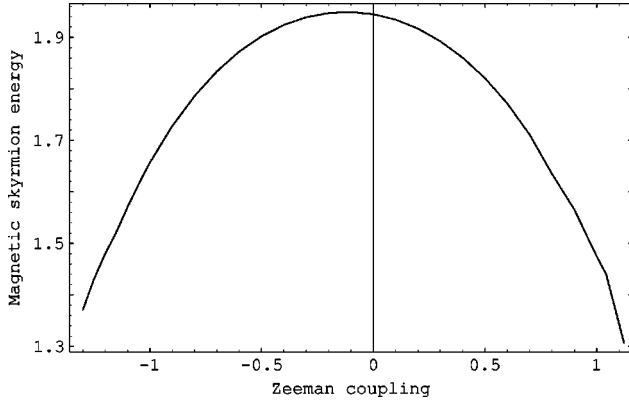


FIG. 7. Energy of the isolated magnetic skyrmion as a function of dimensionless Zeeman coupling  $g$  for  $R/\lambda = 300$ .

vortex phase appears at  $H=0$  and exists for arbitrarily large magnetic field. The Meissner phase, therefore, completely disappears. Vortices become thinner when  $H$  grows. The structure of the vortex core is markedly different from the usual one.

Our analysis in Ref. 19 was entirely based on the simplest possible topological objects: vortices of the usual type. Value of  $\kappa$  for the materials of Wu *et al.*<sup>6</sup> are estimated to be quite large and, consequently, vortices should be heavy compared to magnetic skyrmions. Spontaneously magnetized skyrmion lattice can also occur, as in the previous case of vortices of usual type. Values of  $g$  required to obtain spontaneous vortex state  $g = \ln \kappa$  were very high and made the scenario questionable. This value is lowered to  $g \sim 1$  for magnetic skyrmion lattice.

The free energy per unit length for a single magnetic skyrmion now has form

$$\mathcal{F}_L = \int \rho d\rho \left[ \frac{1}{2} \left( \frac{d\Theta}{d\rho} \right)^2 + \frac{\sin^2 \Theta}{2\rho^2} + \left( \frac{1 + \cos \Theta}{\rho} + a \right)^2 + \left( \frac{a}{\rho} + \frac{da}{d\rho} \right)^2 - g \left( \frac{a}{\rho} + \frac{da}{d\rho} \right) \cos \Theta \right]. \quad (33)$$

The equations read

$$\Theta'' + \frac{1}{\rho} \Theta' = -\frac{\sin \Theta}{\rho} \left( \frac{2 + \cos \Theta}{\rho} + 2a \right) + g \sin \Theta \left( a' + \frac{a}{\rho} \right), \quad (34)$$

$$a'' + \frac{a'}{\rho} - \frac{a}{\rho^2} - a = \frac{1}{\rho} (1 + \cos \Theta) - \frac{g}{2} \Theta' \sin \Theta. \quad (35)$$

We use the same boundary conditions as that for the case of isolated magnetic skyrmion at  $g=0$  (see Sec. IV A). Calculations were performed both for positive and negative values of  $g$ . Plot of the energy of the magnetic skyrmion as a function of  $g$  is presented in Fig. 7. The characteristic feature of this dependence is a maximum near  $g=0$ . Profiles of the magnetic field  $b(\rho)$  for different  $g$  of both signs are presented in Fig. 8. Zeeman interaction strongly influences the behavior of  $b(\rho)$  near the center of the magnetic skyrmion and in quite different manner for positive and negative  $g$ .

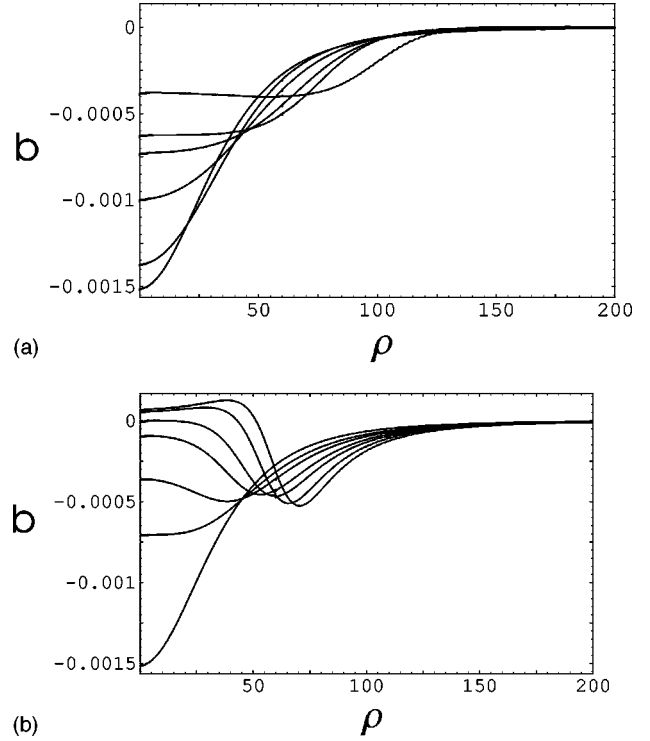


FIG. 8. Magnetic field of the isolated magnetic skyrmion as a function of distance from the center  $\rho$  for different Zeeman coupling and for the case of  $\rho_{\max} = 300\lambda$  (see Fig. 3 caption). (a)  $g = 0, 0.5, 0.7, 0.9, 1.0, 1.1$ . (b)  $g = 0, -0.5, -0.7, -0.9, -1.0, -1.1$ . In both cases a smaller  $|g|$  corresponds to a lower at  $\rho=0$  curve.

Note, however, that as  $|g|$  increases, the behavior of the function changes significantly in the interval of  $\rho$  from the origin up to only some limiting value, after which it remains approximately the same for different  $g$ . Thus we observe that nonzero  $g$  actually introduces new length scale in the problem. Changes in the profile of  $\Theta(\rho)$  with  $g$  are less pronounced and are not displayed.

## VI. DISCUSSION

In this paper we performed topological classification of solutions in  $SO(3)$  symmetric Ginzburg-Landau free energy. This model with addition of very small symmetry breaking terms describes heavy fermion superconductor  $UPT_3$  and possibly other triplet superconductors. A class of topological solutions in weak magnetic field carrying two units of magnetic flux was identified. These solutions, magnetic skyrmions, are nonsingular (do not have singular core as Abrikosov vortices do). They repel each other as  $1/r$  at distances much larger than magnetic penetration depth  $\lambda$  forming relatively robust triangular lattice. At lattice spacings much larger than  $\lambda$  their energy is reduced by a factor of the order of  $\ln \kappa$  as compared to the usual Abrikosov vortex solutions and therefore dominate the magnetic properties for strongly type II superconductors. The lower critical magnetic field  $H_{c1} = \Phi_0/4\pi\lambda^2$  is reduced correspondingly by a factor  $2 \ln \kappa$ .

Magnetization near  $H_{c1}$  instead of sharply rising with infinite derivative increases gradually as  $(H - H_{c1})^2$ . This agrees very well with the experimental results for  $UPT_3$ , see Fig. 1 of Ref. 15. For fields higher than several  $H_{c1}$  London



approximation is not valid anymore since magnetic skyrmions will start to overlap. At distances between fluxons of order  $\lambda$  (or at the field  $H'_{c1} \sim H_{c1} 2 \ln \kappa$ ) one expects that ordinary Abrikosov vortices, which carry one unit of magnetic flux, become energetically favorable. The usual vortex picture has indeed been observed at high fields by Yaron *et al.*<sup>24</sup> Curiously, our result on magnetization is similar to the conclusions of Burlachkov *et al.*<sup>25</sup> who investigated stripelike (quasi-one-dimensional) spin textures in triplet superconductors. Magnetic skyrmions are quite stable objects and they are not destroyed by small perturbations of exact SO(3) symmetry of the original model Eqs. (3)–(5). Moreover, deformed magnetic skyrmions might exist even at large deviations from exact SO(3) symmetry. We demonstrated this including Zeeman-like interaction Eq. (32).

Let us list below the experimental features which can allow the identification of the magnetic skyrmions lattice.

(1) The lower critical field is significantly smaller than usually expected. For such strongly type II superconductors as  $\text{UPt}_3$ ,  $\text{Sr}_2\text{RuO}_4$ , or  $\text{Sr}_2\text{YRu}_{1-x}\text{Cu}_x\text{O}_6$  with  $\kappa \sim 50\text{--}70$  the reduction amounts 8 times. Although  $H_{c1}$  is expected to be very small (less than 1 G) it is still measurable.

(2) Magnetization above  $H_{c1}$ , but below crossover to Abrikosov vortex lattice  $H'_{c1} \sim (\Phi_0/2\pi\lambda^2)\ln \kappa$  is markedly distinct from the usual one due to long range nature of the magnetic skyrmions.

(3) The unit of flux quantization is different:  $2\Phi_0$ .

(4) The magnetic field profile is different: no exponential drop even at very sparse lattices.

(5) Superfluid density  $|\vec{\psi}|^2$  is almost constant throughout the mixed state. There are no normal cores of the fluxons. This can be tested using the scanning tunneling microscopy technique.

(6) Due to the fact that there is no small normal core where dissipation and pinning usually take place, one expects that pinning effects are greatly reduced. Correspondingly, the critical current should be very small.

(7) The vortex lattice in the region around  $H_{c1}$  can melt into the so-called lower field vortex liquid due to thermal fluctuations.<sup>26</sup> The melting of the usual Abrikosov vortex lattice is easy even in not very strongly fluctuating superconductors because the interaction between Abrikosov vortices is exponentially small. This is not so for magnetic skyrmions. Due to their long range  $1/r$  interaction the lattice is more robust and therefore no melting is expected.

#### ACKNOWLEDGMENTS

The authors are grateful to B. Maple for a discussion of the results of Ref. 13, to L. Bulaevskii, T.K. Lee, H.C. Ren, J. Sauls, and M.K. Wu for discussions, and to A. Balatsky for hospitality while at Los Alamos. This work was supported by NSC, Republic of China, through Contract No. NSC86-2112-M009-034T.

<sup>1</sup>K. Machida and T. Ohmi, J. Phys. Soc. Jpn. **67**, 1122 (1998).

<sup>2</sup>J. A. Sauls, Adv. Phys. **43**, 113 (1994).

<sup>3</sup>M. Sigrist and K. Ueda, Rev. Mod. Phys. **63**, 239 (1991).

<sup>4</sup>Y. Maeno, H. Hashimoto, K. Yoshida, S. Nishizaki, T. Fujita, J. G. Bednorz, and F. Lichtenberg, Nature (London), **372**, 532 (1994).

<sup>5</sup>T. M. Rice and M. Sigrist, J. Phys.: Condens. Matter **7**, L643 (1995).

<sup>6</sup>M. K. Wu, D. Y. Chen, F. Z. Chien, S. R. Sheen, D. C. Ling, C. Y. Tai, G. Y. Tseng, D. H. Chen, F. C. Zhang, Z. Phys. B **102**, 37 (1997).

<sup>7</sup>Y. Ren, J. H. Xu, and C. S. Ting, Phys. Rev. Lett. **74**, 3680 (1995).

<sup>8</sup>P. I. Soininen, C. Kallin, and A. J. Berlinsky, Phys. Rev. B **50**, 13 883 (1994); A. J. Berlinsky, A. L. Fetter, M. Franz, C. Kallin, and P. I. Soininen, Phys. Rev. Lett. **75**, 2200 (1995).

<sup>9</sup>D. Chang, C. Y. Mou, B. Rosenstein, and C. Wu, Phys. Rev. Lett. **80**, 145 (1998); Phys. Rev. B **57**, 7955 (1998).

<sup>10</sup>T. A. Tokuyasu, D. W. Hess, and J. A. Sauls, Phys. Rev. B **41**, 8891 (1990).

<sup>11</sup>I. A. Luk'yanchuk and M. E. Zhitomirsky, Supercond. Rev. **1**, 207 (1995).

<sup>12</sup>M. M. Salomaa and G. E. Volovik, Rev. Mod. Phys. **59**, 533 (1987).

<sup>13</sup>A. Amann, A. C. Mota, M. B. Maple, H. von Lohneysen, Phys. Rev. B **57**, 3640 (1998).

<sup>14</sup>Z. Zhao, F. Behroozi, S. Adenwalla, Y. Guan, J. B. Ketterson, B. K. Sarma, and D. G. Hinks, Phys. Rev. B **43**, 13 720 (1991).

<sup>15</sup>A. Knigavko and B. Rosenstein, Phys. Rev. Lett. **82**, 1261 (1999).

<sup>16</sup>M. Tinkham, *Introduction to Superconductivity* (McGraw-Hill, Singapore, 1996).

<sup>17</sup>K. Machida and M. A. Ozaki, Phys. Rev. Lett. **66**, 3293 (1991); T. Ohmi and K. Machida, *ibid.* **71**, 625 (1993); J. Phys. Soc. Jpn. **65**, 4018 (1996).

<sup>18</sup>M. E. Zhitomirsky and K. Ueda, Phys. Rev. B **53**, 6591 (1996).

<sup>19</sup>A. Knigavko and B. Rosenstein, Phys. Rev. B **58**, 9354 (1998).

<sup>20</sup>K. A. Park and R. Joynt, Phys. Rev. Lett. **74**, 4734 (1995).

<sup>21</sup>J. A. Sauls, J. Low Temp. Phys. **95**, 153 (1994).

<sup>22</sup>A. Garg and D. C. Chen, Phys. Rev. B **49**, 479 (1994).

<sup>23</sup>R. Rajaraman, *Solitons and Instantons* (North-Holland, Amsterdam, 1982).

<sup>24</sup>U. Yaron, P. L. Gammel, G. S. Boebinger, G. Aeppli, P. Schiffer, E. Bucher, D. J. Bishop, C. Broholm, and K. Mortensen, Phys. Rev. Lett. **78**, 3185 (1997).

<sup>25</sup>L. I. Burlachkov and N. B. Kopnin, Zh. Éksp. Teor. Fiz. **92**, 1110 (1987) [Sov. Phys. JETP **65**, 630 (1987)].

<sup>26</sup>D. R. Nelson, Phys. Rev. Lett. **60**, 1973 (1988); D. S. Fisher, M. P. A. Fisher, and P. A. Huse, Phys. Rev. B **43**, 130 (1991).